Experimental Characterization of Fault Impacts on the Functioning Variables of an Inverter Driven Heat Pump

Derek Noel, Philippe Riviere, C. Teuillieres, O. Cauret, D. Marchio

Experimental Characterization of Fault Impacts on the Functioning Variables of an Inverter Driven Heat Pump

D.Noël[1, 2], P. Rivière[2], C.Teuillières[1], O. Cauret[1], D. Marchio[2]

(1) EDF Lab Les Renardières, Ecuelles, France

(2) Centre for Energy Efficiency of Systems (CES), Mines ParisTech, PSL Research University, Paris, France

1. ABSTRACT

The heat pump technology answers to the three key targets of the European Union climate action by reducing greenhouse gas emissions, increasing renewable energy share and improving energy efficiency of buildings. In standard conditions, heat pumps can reach very high coefficients of performance (COPs). However, the in-situ COPs are poorly known and they depend on many factors such as sizing, climate, quality of installation, and can also be affected by some abnormal functioning caused by faults, such as heat exchanger fouling or incorrect refrigerant charge. This paper focuses on the characterization of these faults for an inverter driven residential heat pump, for which literature is very limited, in order to be able to detect those as early as possible, and thus to facilitate maintenance operation. A series of experimental tests has been conducted to generate correlations between faults and their impact on the main functioning variables and performances. The test results obtained are presented and discussed. Further steps required to develop an operational automated fault detection and diagnostic method for inverter driven heat pumps are finally discussed, as well as the possibility to associate it with a performance assessment method for heat pumps that was previously developed and validated.

Keywords: Heat pump, Inverter, Fault impact, Characterization

2. INTRODUCTION

Heat pumps (HP) contribute to reducing heating energy consumption in dwellings. But their performances depend on many external factors and can be impacted by different kinds of faults. These can be caused by a control issue, or by a physical deviation of the thermodynamic cycle as compared to its original or intended design. This study concerns this second kind of faults, which are difficult and expensive to diagnose (Li & Braun, 2009), like heat exchangers fouling and refrigerant under- and over-charging.

The impacts of these faults on the functioning and performance variables of heat pumps have been studied before, Mehrabi and Yuill (2017a & 2017b) made a very complete synthesis of these works by gathering the experimental data of many laboratory experiments. Their work provides generalized relationships between faults intensities (FI) and performance variables, and it shows that there is a remarkable similarity of results from different systems in many cases. Regression coefficients are provided for three different operating conditions in heating mode for charge variations and condenser fouling faults. These conditions are standard test conditions in heating mode (outdoor temperatures 8.33, 1.67 and -8.33 °C for an indoor temperature of 21.1 °C (H1, H2 and H3 from ANSI/AHRI Standard 210/240, 2008). This standard is for air to air and return inlet indoor temperature is fixed. There is little information on air to water and noting on heat pumps with inverter and variable water loop temperature.

This study concerned only fixed-speed HP with fixed orifice (FXO) or thermostatic (TXV) expansion valves. Thus, it is necessary to extend the knowledge of the impacts of faults on inverter-driven heat pumps using an electronic expansion valve (EEV).

Furthermore, a performance assessment method adapted to any type of residential HP has been identified (Tran et al., 2013), improved (Niznik, 2017) and widely validated (Noël et al., 2018). It was made to measure precisely and continuously the performances of heat pumps, particularly air-to-air, without interfering with the normal functioning of the system. It is based on a virtual mass flow sensor from the compressor energy balance, and uses only light instrumentation on the refrigerant side, in order to be easily implemented on-site. This method is able to measure the performances of residential heat pumps in a very large scale of operating conditions, and can thus measure the decrease of performance caused by faults. It measures continuously the refrigerant mass flow rate, which can be very useful in order to detect and/or discriminate between different faults.

This experimental study focuses on quantifying the normalized impacts of faults on different performance and functioning variables as a function of the fault intensity. In particular, the knowledge of the system behaviour under faulty conditions will lead to the identification of the necessary measurements to detect faults at an early stage. Then, this analysis will allow to evaluate in which way the in-situ performance assessment method can be used for fault detection process.

3. EXPERIMENTAL SETUP

3.1 Test bench

The test bench was an air-to-water HP with an inverter-driven rotary-type compressor using R134a as a working fluid, installed in adjacent climatic chambers, where temperature and humidity are controlled. It uses a plate heat exchanger as a condenser, and an electronic expansion valve (EEV). There is no liquid receiver after the condenser.

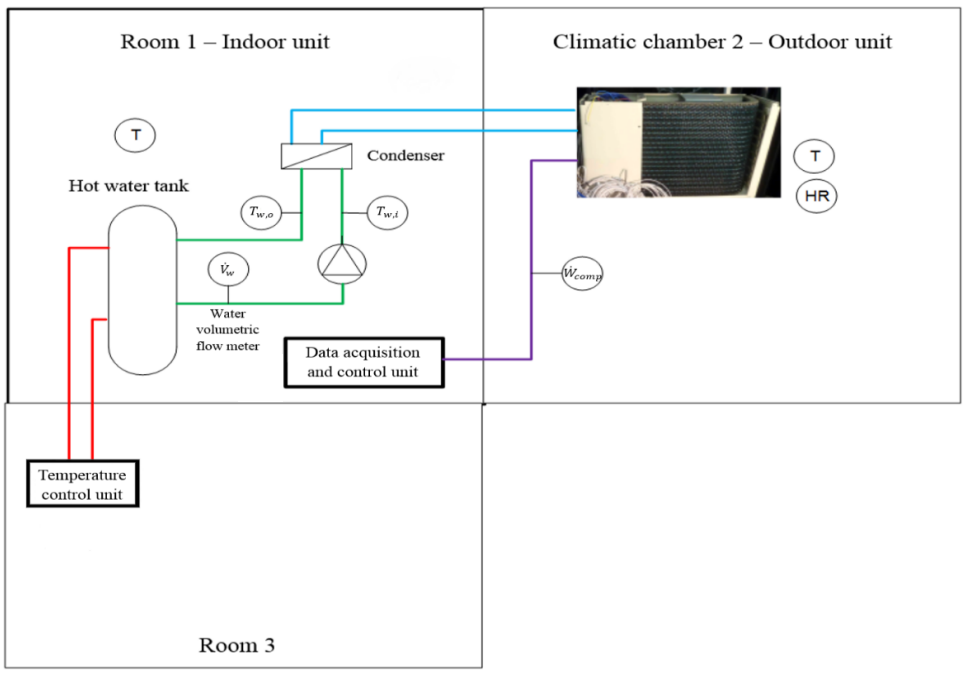

Figure 1: Air-to-water HP installed in climatic chambers

For each measurement condition, the acquisition lasted for two hours in order to be sure that the steady state was reached and to have a sufficient amount of data to analyse. The experimental set-up is described in figure 1.

3.2 Measurements

On the water-side, condenser inlet and outlet water temperatures ($T_{w,in}$ and $T_{w,out}$) were measured, as well as the water volumetric flow rate, $\dot{V}_w$. On the refrigerant side, condenser inlet and outlet temperatures ($T_{cond,in}$ and $T_{cond,out}$), compressor suction and discharge temperatures and pressures (T_{suc}, T_{dis} and P_{suc}, P_{dis}), as well as the compressor frequency (Freq) and EEV opening (EEV) were measured. Temperatures are measured with insulated contact Pt100. Evaporating and condensing temperatures (T_{evap} and T_{cond}) are calculated from P_{suc} and P_{dis}. The refrigerant mass flow rate ($\dot{m}$) is measured thanks to the virtual mass flow rate sensor used in the performance assessment method, using the energy balance of the compressor:

$$\dot{W}_{comp} = \dot{m}\left[(1 - C_{oil})\left(h_{r,comp,o} - h_{r,comp,i}\right) + C_{oil}.c_{p,oil}(T_{dis} - T_{suc})\right] + \dot{Q}_{losses} \qquad (1)$$

Where $\dot{W}_{comp}$ is the compressor power input measured, and $\dot{Q}_{losses}$ the compressor heat losses that are estimated through a measurement of the temperature of the compressor shell surface (Niznik, 2017) and the ambient temperature. The working fluid is mainly composed of refrigerant fluid, but there is also a small part of oil, necessary to ensure the good working of the compressor, that migrates into the refrigerant cycle. The oil fraction, C_{oil}, is considered to be equal to 0.5 % of the total working fluid (Goossens, 2017). Therefore, the enthalpy variation is decomposed into the refrigerant variation of enthalpy and the oil variation of enthalpy. $h_{r,comp,i}$ and $h_{r,comp,o}$ are respectively the refrigerant compressor inlet and outlet enthalpies, $c_{p,oil}$ is the oil specific heat capacity, $T_{comp,i}$ and $T_{comp,o}$ are respectively the compressor inlet and outlet temperatures.

Goossens (2016 and 2017) and Niznik (2017) developed a method to estimate the heat losses of the compressor, based on CFD modelling of different types of compressors and experimental study. This work established the best locations for temperature sensors for the compressor shell and the ambient air and identified the best heat exchange correlations in order to estimate the compressor heat losses.

For rotary compressors, only one surface temperature sensor is necessary on the compressor shell, and only two for scroll compressors (one is used to check the validity of the correlation domain). The surface temperature is referred as T_{surf}. Niznik (2017) concluded that the best solution for the ambient air temperature T_{amb} as seen from the compressor is to measure $T_{amb} = T_{ext}$, with T_{ext} the air temperature outside the HP outdoor unit.

For example, the correlation used to calculate the compressor heat losses for a rotary type compressor is:

$$\dot{Q}_{losses} = \left(\frac{\overline{Nu}_L k}{L} A_L + \frac{\overline{Nu}_{D,1} k}{D} A_D + \frac{\overline{Nu}_{D,2} k}{D} A_D\right)\left(T_{surf} - T_{amb}\right) + \sigma A_{tot}\left(T_{surf}^4 - T_{amb}^4\right) \qquad (2)$$

Where Nu is the Nusselt number for the different sides of the compressor, k is the thermal conductivity of the air, L, D and A stand for the different characteristic dimensions of the compressor, respectively length (height), diameter (1 and 2 for the top and the bottom surface respectively) and area for the lateral side, the top and the bottom of the compressor, σ is the Stefan-Boltzmann constant for radiative heat transfer.

Therefore, the refrigerant mass flow rate can be expressed as:

$$\dot{m} = \frac{\dot{W}_{comp} - \dot{Q}_{losses}}{(1 - C_{oil})(h_{r,comp,out} - h_{r,comp,in}) + C_{oil}.c_{p,oil}(T_{cond,in} - T_{cond,out})} \quad (3)$$

To have the enthalpy values needed, pipe surface temperature measurements are monitored, and if there is no pressure sensor, low and high pressures can be determined from the temperature measurements where the fluid state is undoubtedly diphasic: the evaporator inlet for low pressure and the center of the condenser surface for high pressure. The pressure measurement error that could be caused by the temperature glide of zeotropic fluids classically used in residential HP (R410A, R407C) is very limited (Tran, 2012).

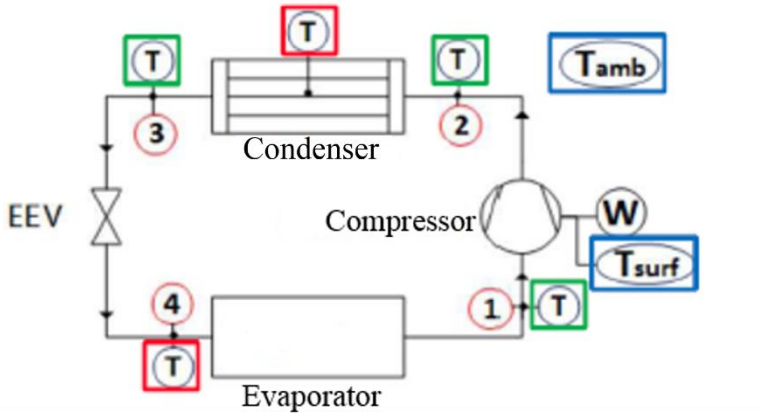

Figure 2: Required measurements for the in-situ performance assessment method

The measurement uncertainty of the refrigerant mass flow rate with this method is estimated to about 5 % maximum, taking into account that the measurement uncertainty for the temperatures is 0.8 K, for the electrical power measurement 0.2 %, for high and low pressures 0.25 %. From the pressure measurements, the absolute measurement uncertainties for condensing and evaporating temperatures are about 0.1 °C.

3.3 Control

The HP unit is controlled with a linear heating curve that sets the leaving water temperature as a function of the outdoor temperature (T_{ext}):

$$T_{w,out} = 45 - T_{ext}\ (°C) \quad (4)$$

The frequency of the compressor is thus controlled with a PI controller in order to provide enough power to maintain the outlet water temperature according to the heating curve.

In a real building, the water circulates through a heating circuit to heat the building, and the water temperature decreases according to the heat losses of the building. Here, these losses are simulated thanks to a water temperature control unit, so the condenser water inlet temperature is set according to the heat losses equation:

$$P_{th} = G.V.(T_{in} - T_{ext}) \quad (5)$$

G=0.6 W/m^{3}K is the overall heat loss coefficient of the virtual building, V=200 m^3 is its volume, T_{in} is the indoor ambient air temperature that would be set inside the building, it was set to 20°C. P_{th} is the heat lost by the building, but it is also the heating power that the HP should provide:

$$P_{th} = \rho_w.\dot{V}_w.c_{p,w}.(T_{w,out} - T_{w,in}) \quad (6)$$

Where ρ_w is the water density, $c_{p,w}$ is its specific heat. The HP provides the heat power needed to make the water temperature go from $T_{w,in}$ to $T_{w,out}$.

The EEV is controlled by a PI controller to maintain the suction superheat to a constant value of 10 °C.

T_{ext}	T_{in}	P_{th}	T_{wout}	T_{win}
10 °C	20 °C	1200 W	35 °C	32.2 °C
5 °C	20 °C	1800 W	40 °C	35.8 °C
0 °C	20 °C	2400 W	45 °C	39.4 °C
-3 °C	20 °C	2760 W	48 °C	41.6 °C

Table 1: Heat power and water temperatures for each outdoor temperature tested

3.4 Test program

Different refrigerant charge were adjusted to simulate over and under charge. Evaporator fouling faults were simulated by reducing the fan speed in order to reduce the air flow rate, as it would be the effect of a real fouling. In the same way, for condenser fouling faults, the water circulating pump was slowed down. Fault levels (i.e. the severity of the faults) are quantified using fault intensity (FI), defined by Yuill and Braun (2013):

$$FI_{CH} = \frac{m_{actual} - m_{nominal}}{m_{nominal}} \quad (7)$$

$$FI_{EA} = \frac{\dot{V}_{air,actual} - \dot{V}_{air,nominal}}{\dot{V}_{air,nominal}} \quad (8)$$

$$FI_{CA} = \frac{\dot{V}_{w,actual} - \dot{V}_{w,nominal}}{\dot{V}_{w,nominal}} \quad (9)$$

Where m is refrigerant mass, $\dot{V}_{air}$ is the air volumetric flow rate through the evaporator and $\dot{V}_{w}$ is the water volumetric flow rate through the condenser.

Three types of faults were studied:

Type of fault	FI tested [-]
Refrigerant mischarge	+0.1, 0, -0.1, -0.3, -0.5
Evaporator fouling	0, -0.1, -0.2, -0.3, -0.4, -0.5
Condenser fouling	0, -0.1, -0.2, -0.3, -0.4, -0.5

Table 2: Fault Intensities tested

The ranges of FI were chosen in order to be sure that a significant impact could be observed, at least for the strongest fault intensities.

Each FI was tested under 4 different outdoor temperatures: 10 °C, 5 °C, 0 °C and -3 °C.

4. RESULTS

The impacts of faults on the operating and performance variables are quantified using the fault impact ratio (FIR) defined by Yuill and Braun (2013), and extended to other variables: the coefficient of performance (COP), the discharge pressure (P_{dis}), refrigerant mass flow rate (m), compressor frequency (Freq), the EEV opening (EEV), subcooling (SC), condensing and evaporating temperatures (T_{cond} and T_{evap}), the air temperature at the evaporator outlet (T_{airout}).

The measurement uncertainties are represented with error bars on the graphs, slightly shifted from the data points when it improves readability, and not represented when negligible.

$$FIR_{COP} = \frac{COP_{actual}}{COP_{unfaulted}} \quad (10)$$

$$FIR_{m} = \frac{\dot{m}_{actual}}{\dot{m}_{unfaulted}} \quad (11)$$

$$FIR_{Freq} = \frac{Freq_{actual}}{Freq_{unfaulted}} \quad (12)$$

$$FIR_{EEV} = \frac{EEV_{actual}}{EEV_{unfaulted}} \quad (13)$$

$$Residual_{SC} = SC_{actual} - SC_{unfaulted} \quad (14)$$

$$Residual_{Tcond} = T_{cond,actual} - T_{cond,unfaulted} \quad (15)$$

$$Residual_{Tevap} = T_{evap,actual} - T_{evap,unfaulted} \quad (16)$$

$$Residual_{Tairout} = T_{airout,actual} - T_{airout,unfaulted} \quad (17)$$

4.1 Impact of the refrigerant charge

The mass of fluid chosen as "nominal" (FI_{CH} = 0) was not necessarily the optimal charge, as it can be observed in some following figures. It remains interesting to observe the impact of the variation of the refrigerant charge.

The results can partly be compared with those obtained by Mehrabi and Yuill (2017a), mentioned as MY2017 in the graphics, to see if there are similarities between fixed-speed and inverter driven HP.

For the strongest charge fault (FI_{CH} = -0.5), at 0 °C and -3 °C, the HP was only dealing with frost and defrosting cycles, thus those points are not always exploitable.

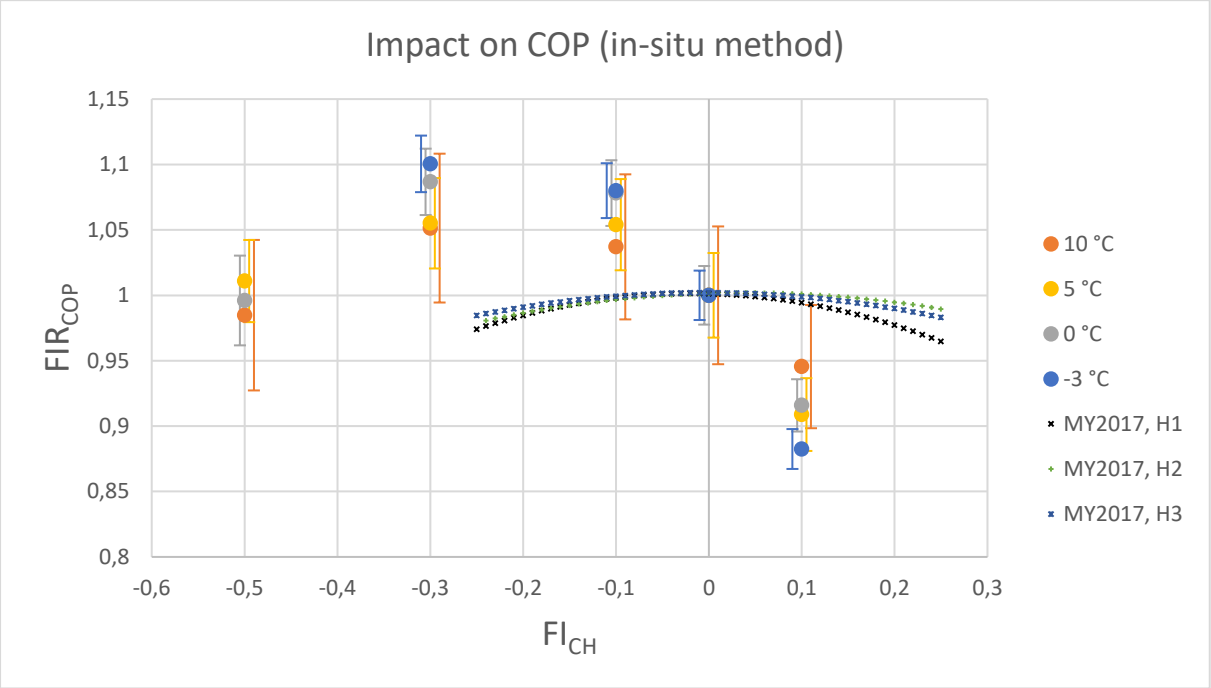

Figure 3: Refrigerant charge impact on the COP, compared with Mehrabi & Yuill (2017a)

In Figure 3, we can see that a refrigerant overcharge leads to a reduction of the performances, especially for low outdoor temperatures, as well as for a strong undercharge. The trends are the same for every outdoor temperature, but the measurement uncertainty at 10 °C is too high to observe a significant impact.

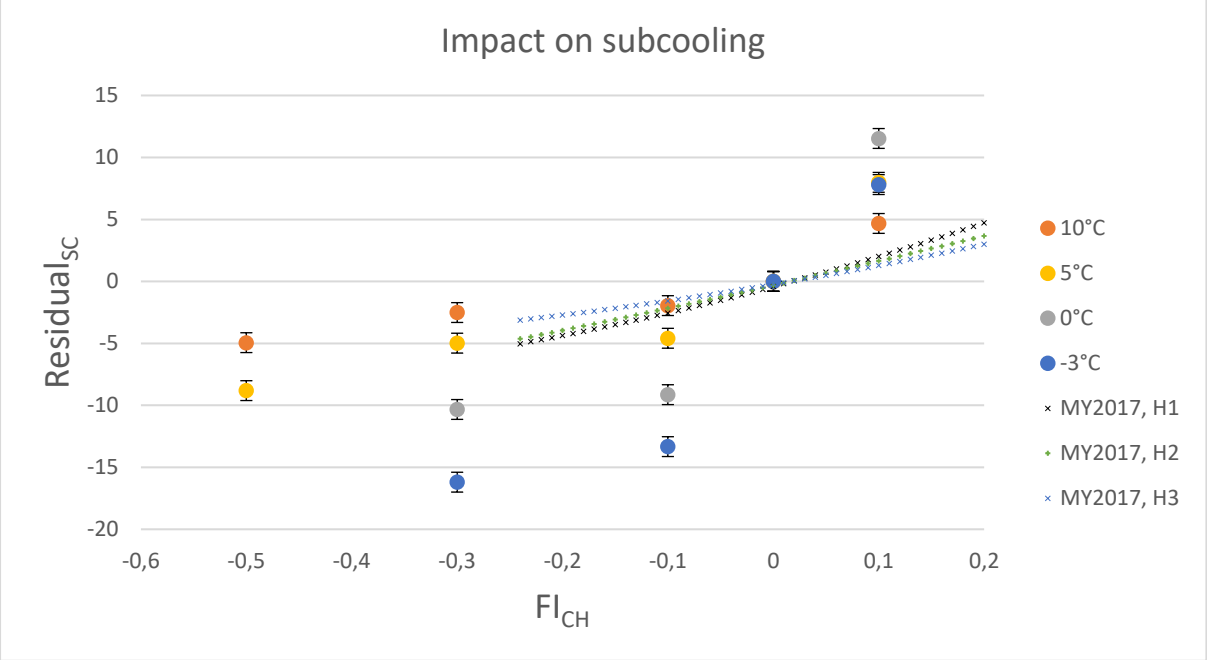

Figure 4: Refrigerant charge impact on subcooling, compared with Mehrabi & Yuill (2017a)

As figure 4 shows, subcooling is strongly and significantly impacted by refrigerant charge faults, for every climate condition tested. It decreases as the mass of refrigerant decreases. Actually, for the strongest fault (FI_{CH} = -0.5), the fluid is even diphasic at the condenser outlet, for every climate condition. The curves obtained from the regression coefficients given in Mehrabi & Yuill (2017a) show the same trends, even though the systems are different, with a fixed-speed compressor and a thermostatic expansion valve. The three conditions tested (H1, H2 and H3) are standard test conditions (ANSI/AHRI Standard 210/240, 2008). The effect on subcooling is more pronounced for the variable speed HP. It can be explained looking at the evolution of other parameters. Figure 5 highlights the influence of refrigerant charge on condensing temperature, very similar to the influence on subcooling. Figures 6, 7 and 8 show how the HP reacts to a lack of refrigerant in order to compensate: the compressor speed increases, the EEV opens and thus the refrigerant mass flow rate increases. Then, the mass flow rate increase amplifies the impact of reducing high pressure on subcooling value. Conversely, in Mehrabi and Yuill (2017a), the effects are contradictory, as there is no action of the compressor in order to compensate the loss of heating power: the mass flow rate decreases in case of lack of refrigerant and limits the impact of reducing high pressure on subcooling.

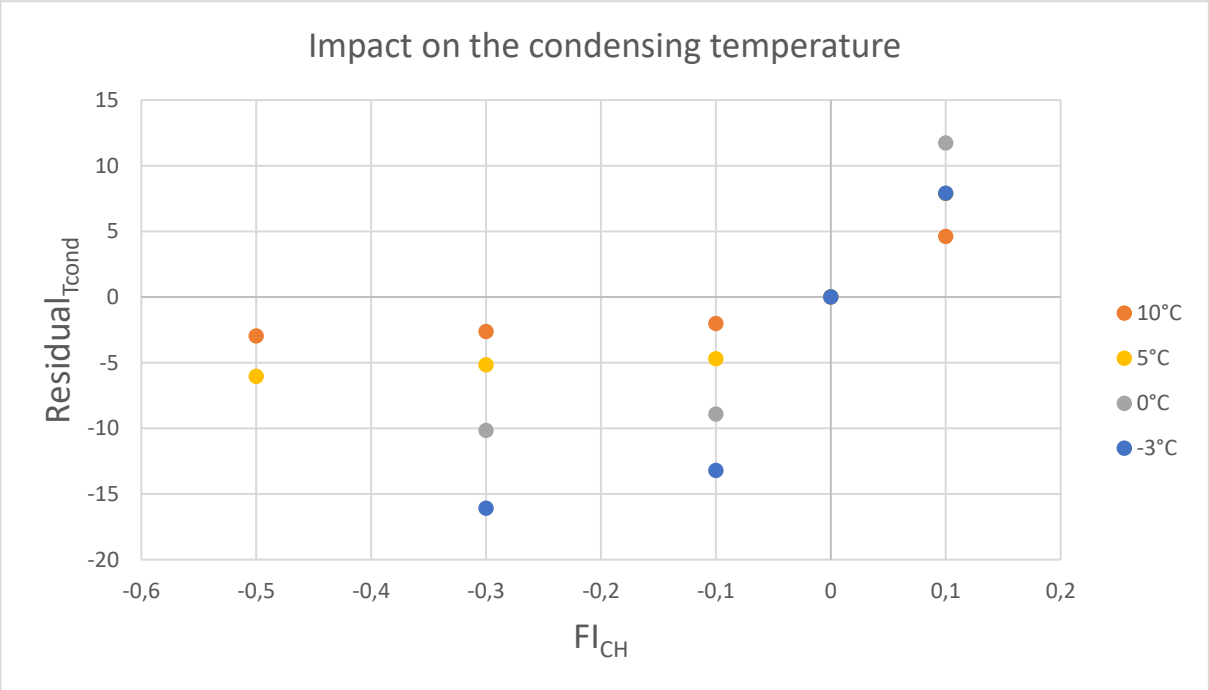

Figure 5: Impact of refrigerant charge on the condensing temperature

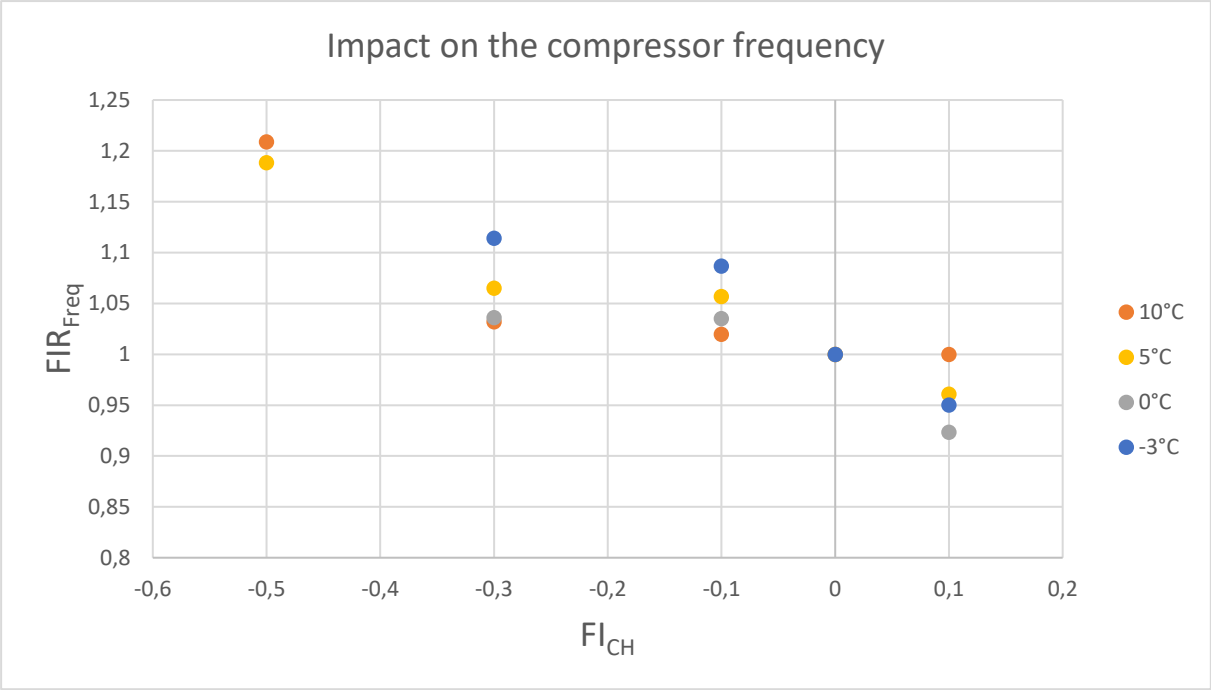

Figure 6: Impact of refrigerant charge on the compressor rotating frequency

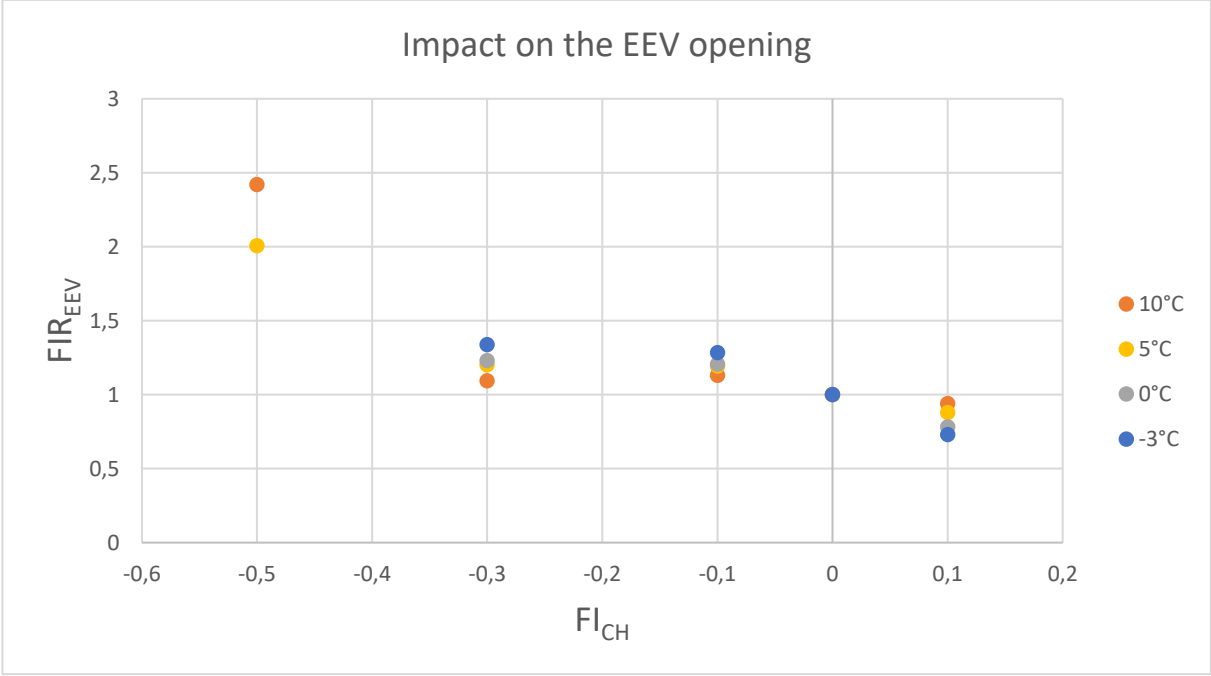

Figure 7: Impact of refrigerant charge on the EEV opening

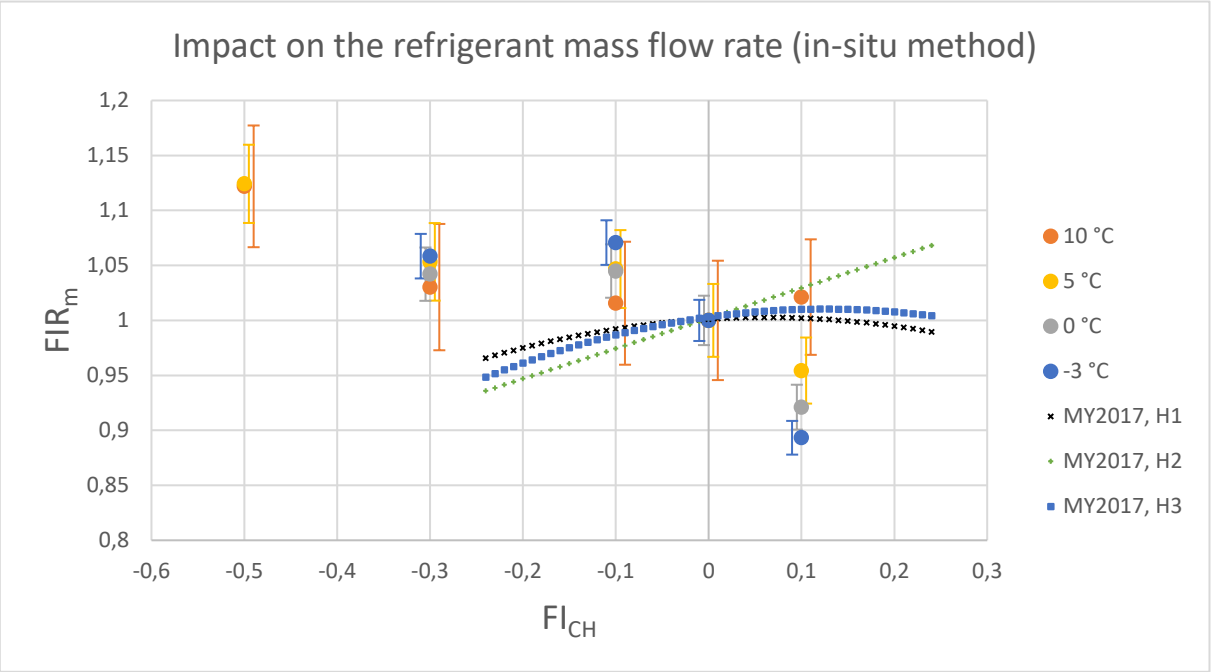

Figure 8: Impact of refrigerant charge on the refrigerant mass flow rate

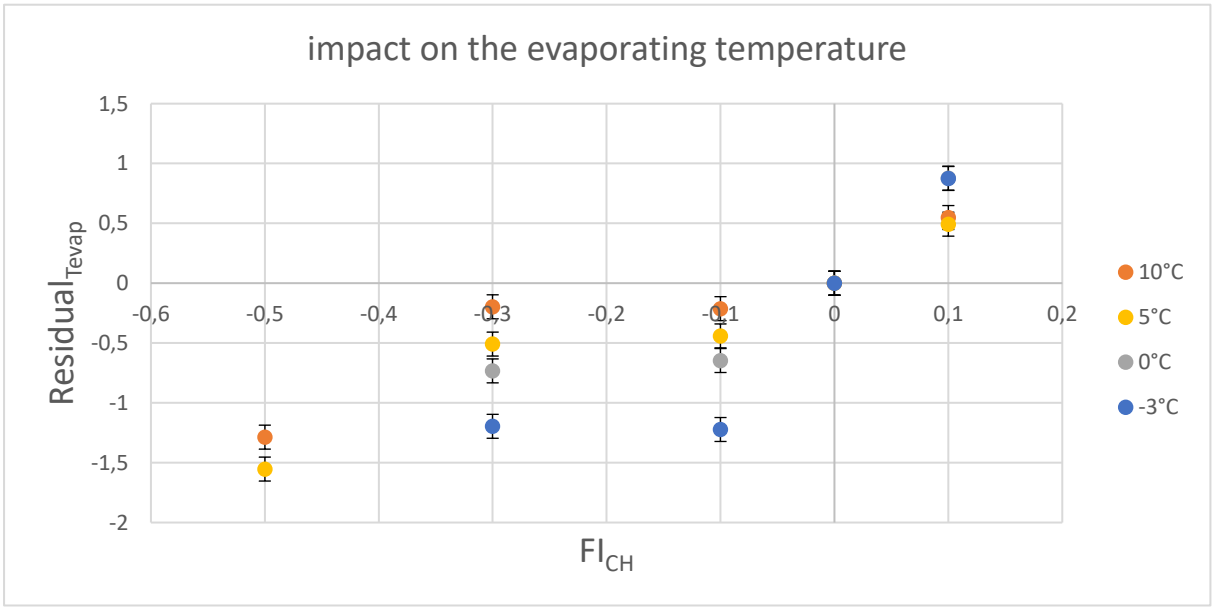

Figure 9: Impact of refrigerant charge on the evaporating temperature

The evaporating temperature increases a little as the refrigerant charge increases and conversely, decreases in case of lack of charge. It can explain why the tested heat pump was only dealing with frost and defrost cycles in case of low outside conditions.

It means that another interesting effect of refrigerant undercharge is that it can reduce the range of outdoor temperatures under which the HP can operate. Also, an overcharge leads to a higher discharge pressure and temperature and can reach safety limits at low outdoor temperatures.

4.2 Impact of evaporator fouling faults

The COP was calculated without taking into account the consumption of the fan, because it decreases as the fan speed decreases, which is not representative of a real fouling effect.

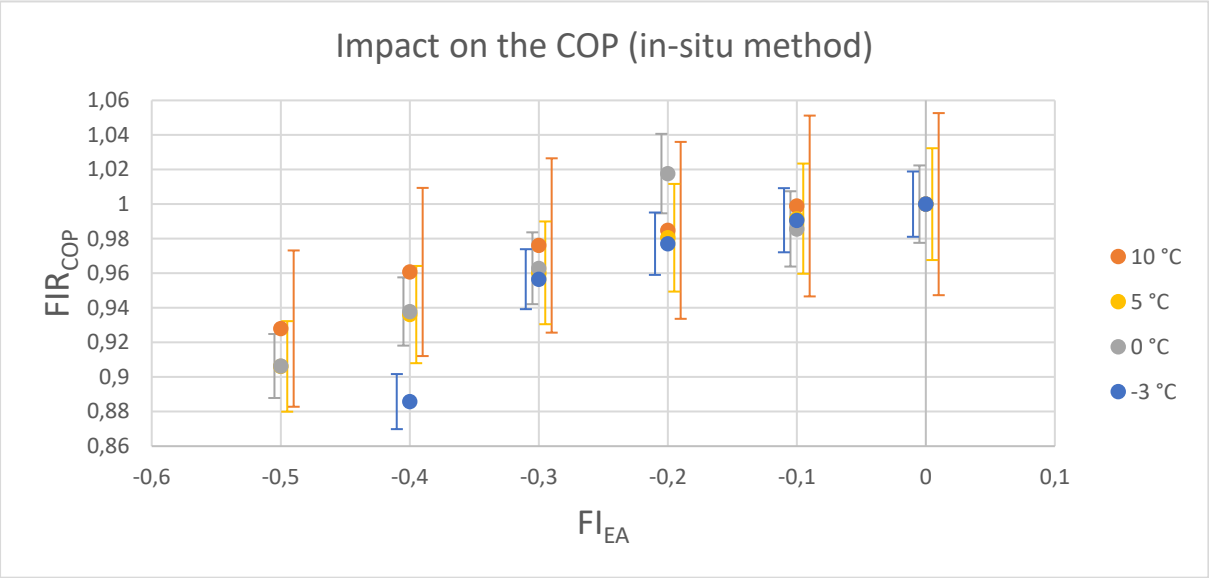

Figure 10: Impact of evaporator fouling on the COP

Figure 10 shows how reducing the air flow rate at the evaporator can affect the performances of the HP. The impact becomes significant only for the strongest FIs, especially at 10 °C for which the measurement uncertainty is not negligible.

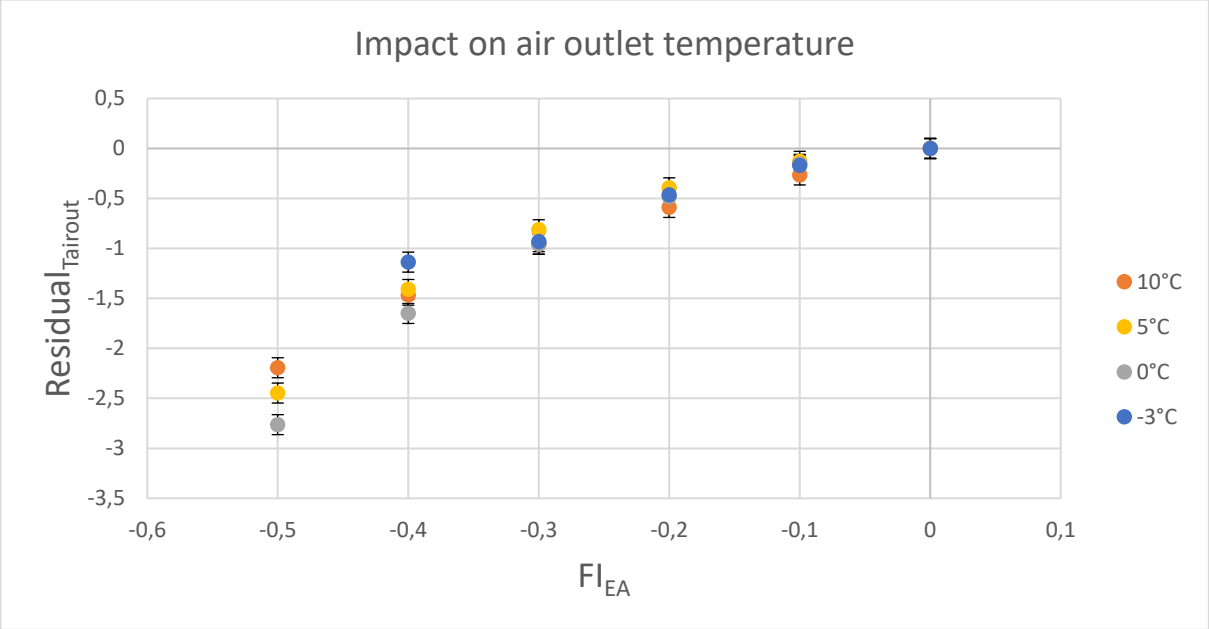

Figure 11: Impact of evaporator fouling on the air outlet temperature at the evaporator

Obviously, reducing the air flow rate at the evaporator has a direct impact on the air temperature at the evaporator outlet. This could be an easy and interesting measurement to make in order to detect this kind of fault.

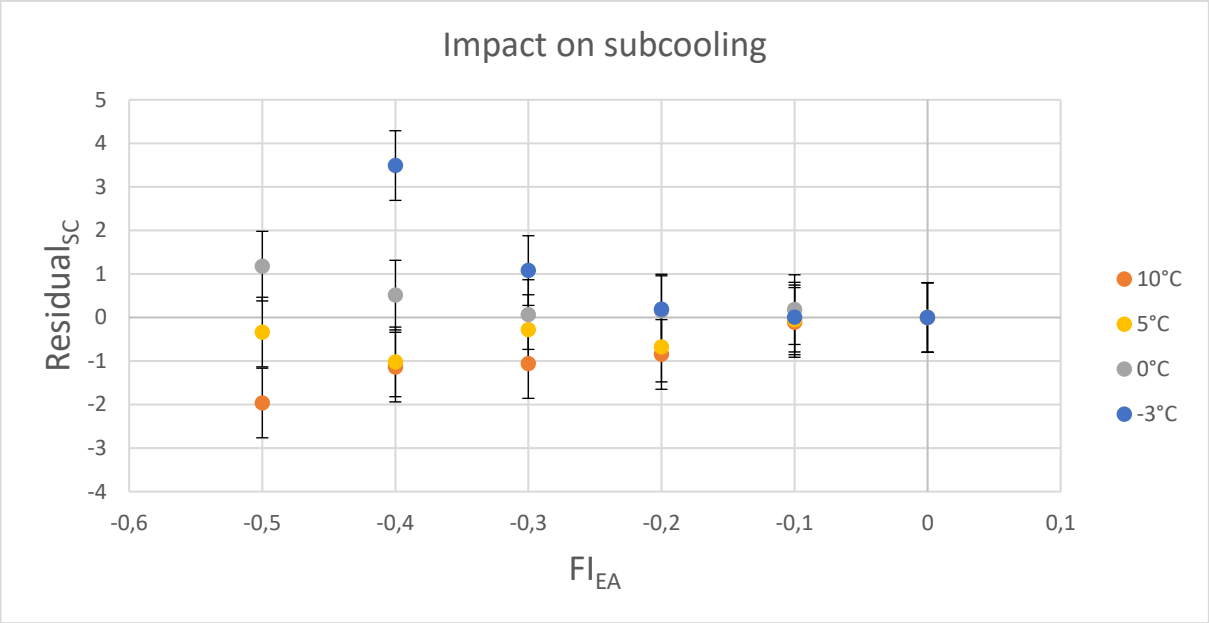

Figure 12: Impact of evaporator fouling on subcooling

As opposed to refrigerant charge variation, the effect of the reduction of the air flow rate at the evaporator on subcooling depends on the operating conditions. It increases with the reduction of air flow rate at low outdoor temperatures and decreases for higher outdoor temperatures. It is almost not affected at 5°C.

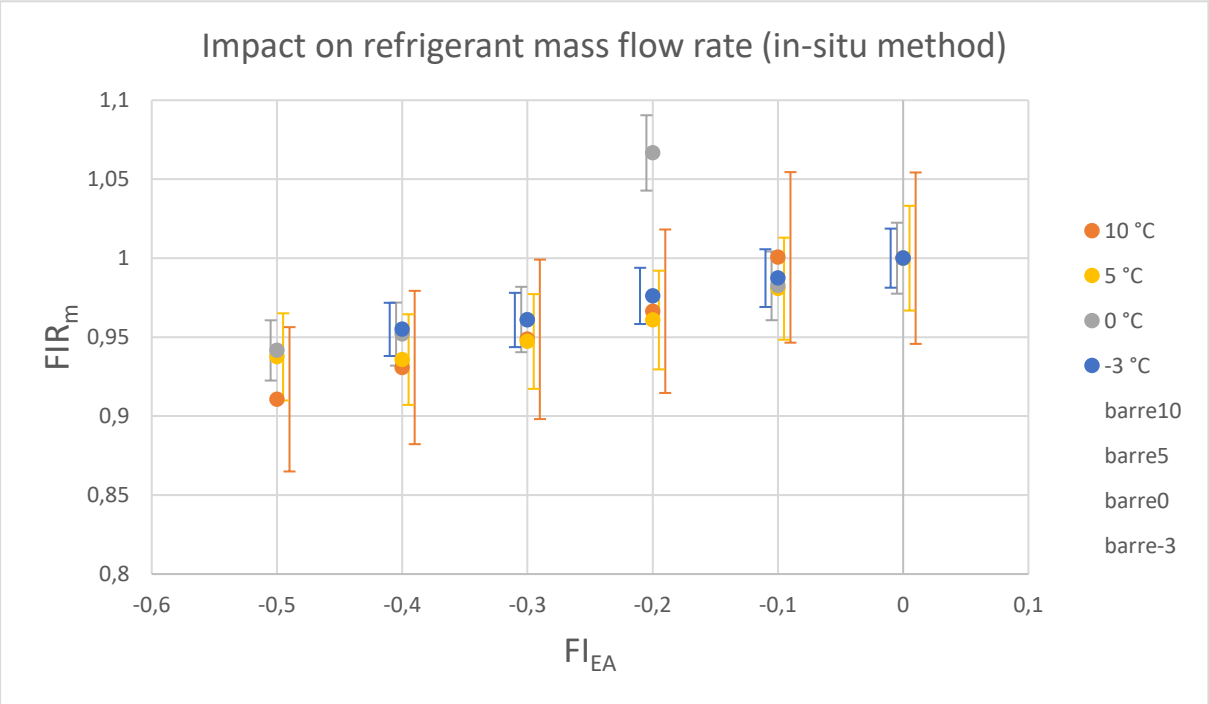

Figure 13: Impact of evaporator fouling on the refrigerant mass flow rate

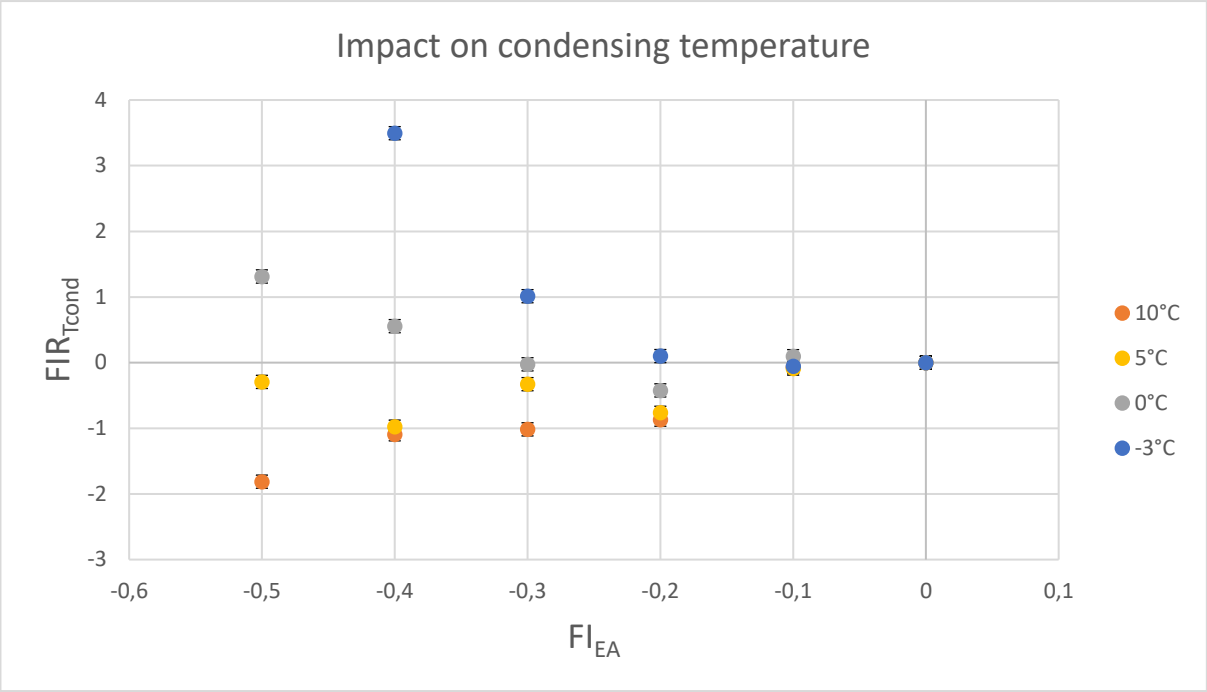

Figure 14: Impact of evaporator fouling on the condensing temperature

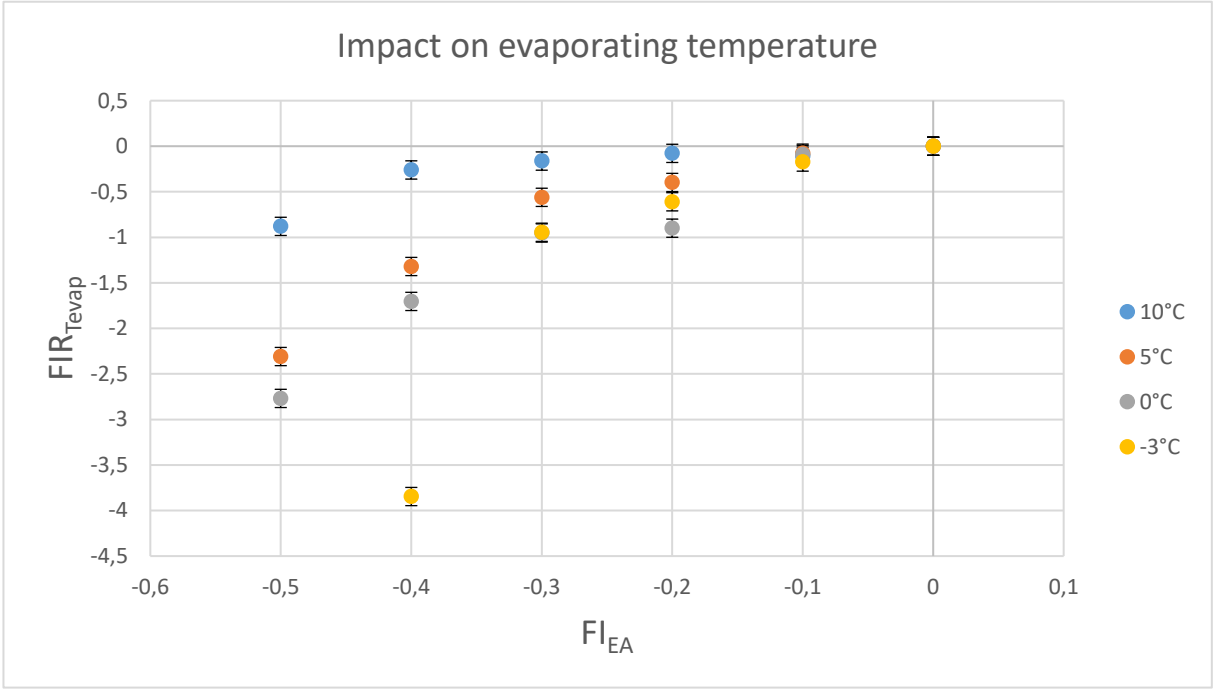

Figure 15: Impact of evaporator fouling on the evaporating temperature

As could be expected, evaporator fouling causes a decrease of the evaporating temperature for every climate condition tested.

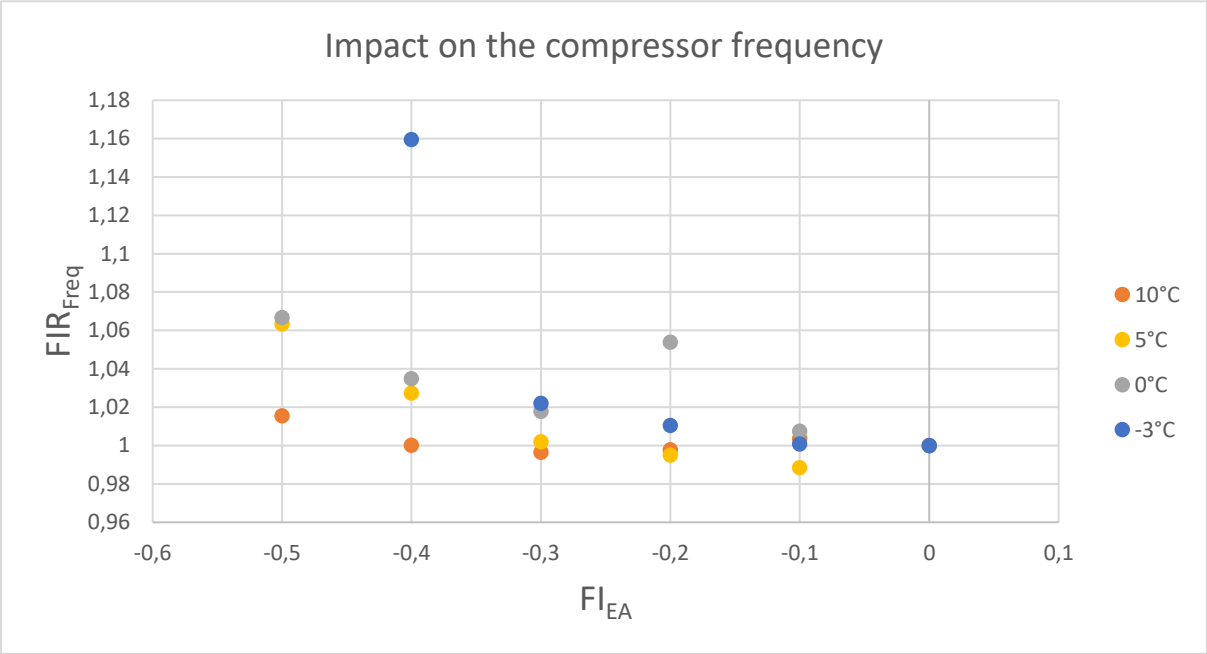

Figure 16: Impact of evaporator fouling on the compressor rotating frequency

The compressor frequency increases a little with the decrease of the air flow rate at the evaporator in order to maintain the heating power constant.

As the evaporating temperature decreases with the FI, the fluid density becomes lower. This explains the small decrease in refrigerant mass flow rate that is not fully compensated with the moderated increase in compressor frequency.

4.3 Impact of condenser fouling faults

The COP does not take into account the consumption of the circulating pump, because it decreases as the pump speed decreases, which is not representative of a real fouling effect.

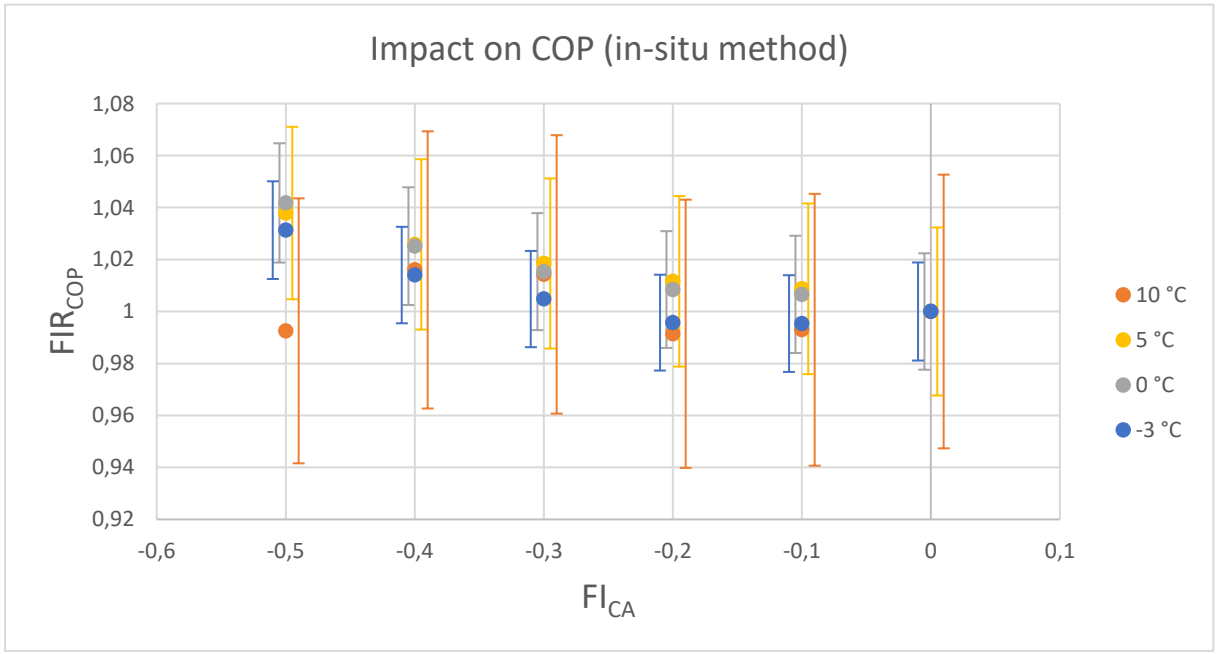

Figure 17: Impact of condenser fouling on the COP

The COP is only very lightly impacted by the condenser fouling, especially taking into account the measurement uncertainties. It shows that a variable speed HP can compensate faults to some extent. It also shows that maybe the circulating pump consumption could be reduced for high outdoor temperature and low load. Also, the small increase in the COP can be explained by the fact that in order to compare the results for the same heating capacity, as the circulating pump was slowed down, the condenser water inlet temperature was decreased. This lead to reduce the condensing temperature, as can be seen in figure 21, which contributes to a better value of COP. This is not necessarily representative of a real fouling effect, the results should then be taken carefully.

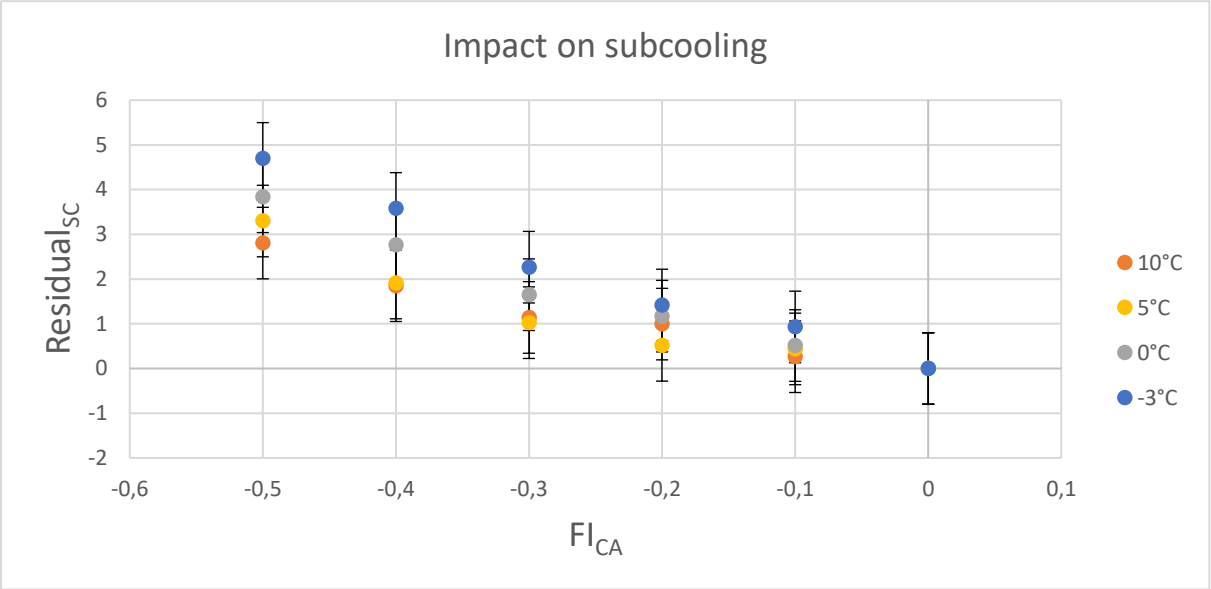

Figure 18: Impact of condenser fouling on subcooling

The effect of condenser fouling on subcooling is significant for every outdoor temperature. As opposed to the case of the lack of refrigerant, subcooling increases when the flow rate through the condenser decreases.

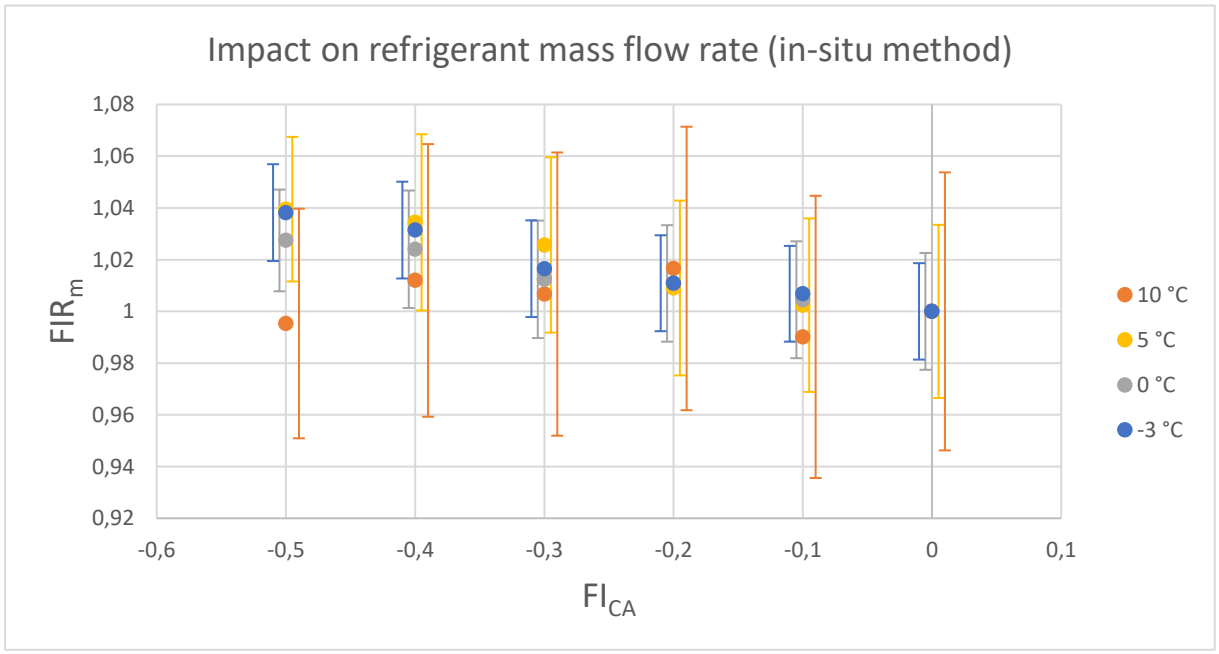

Figure 19: Impact of condenser fouling on the refrigerant mass flow rate

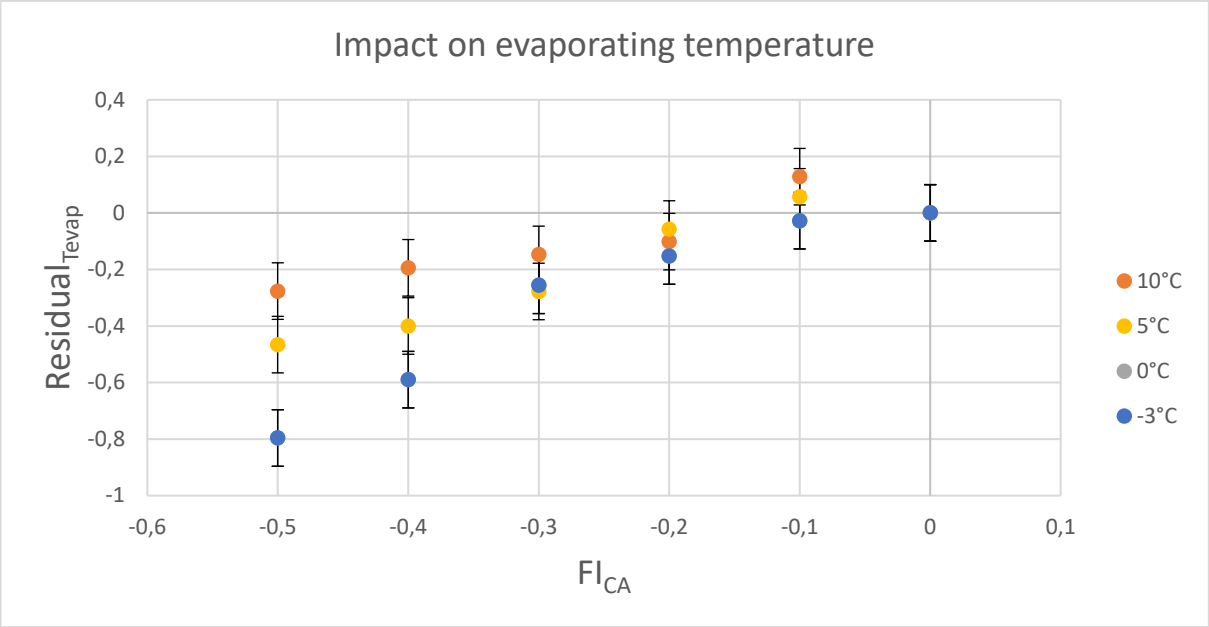

Figure 20: Impact of condenser fouling on the evaporating temperature

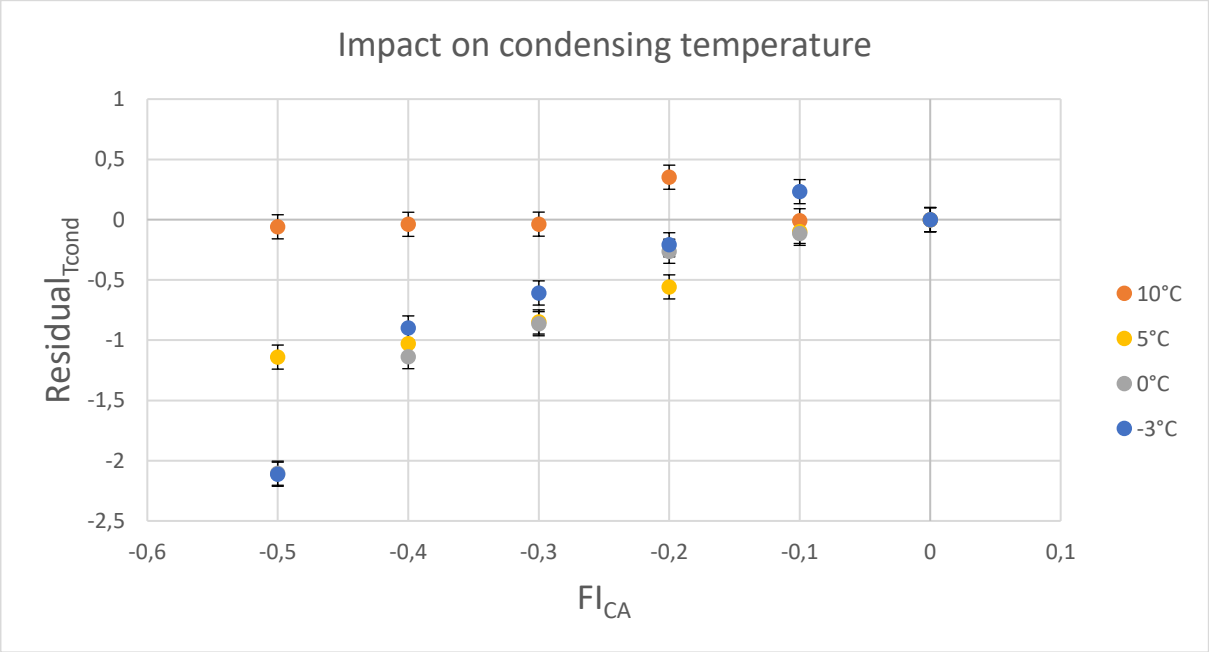

Figure 21: Impact of condenser fouling on the condensing temperature

Figure 20 shows that the reduction of the water flow rate through the condenser reduces the evaporating temperature, but not very significantly. However, figure 21 shows that the condensing temperature is strongly impacted for every temperature below 10°C.

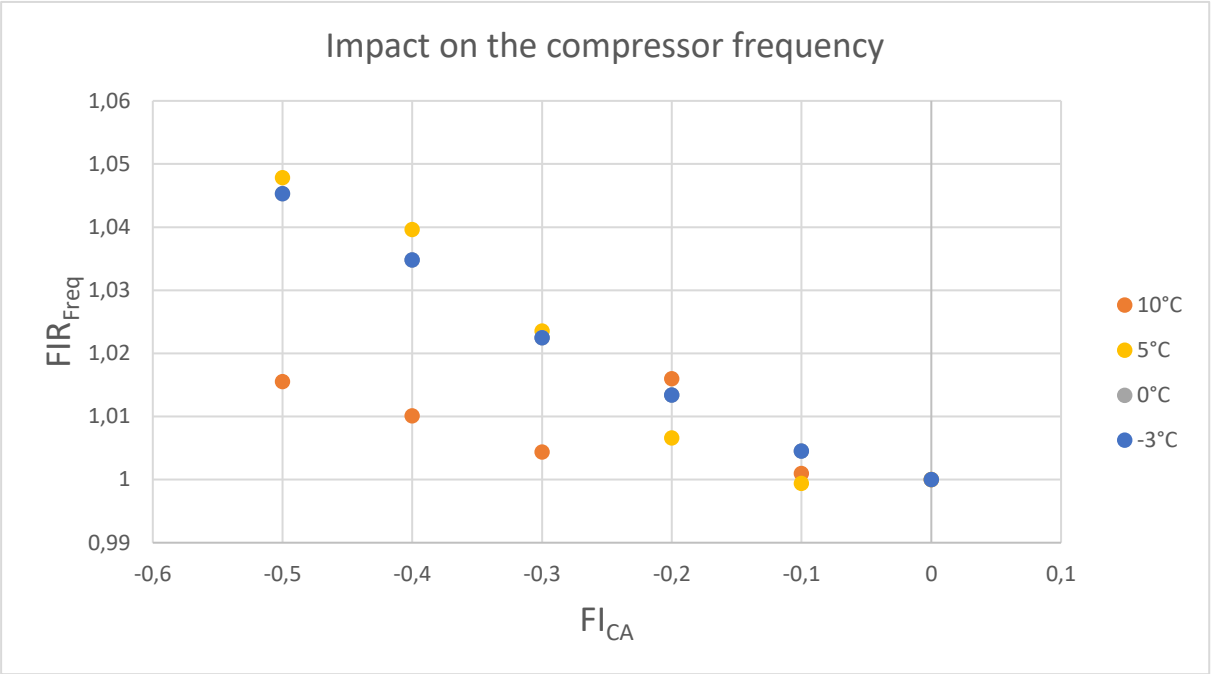

Figure 22: Impact of condenser fouling on the compressor rotating frequency

The compressor frequency increases a little with the decrease of water flow rate through the condenser as figure 22 shows, which is in accordance with the increase of refrigerant mass flow rate observed in figure 19, even though thos two effects are not very significant.

5. DISCUSSION

The following table is a short summary of the significant impacts of faults on the functioning variables of the inverter-driven HP studied, considering the measurement uncertainties:

	Refrigerant charge reduction	Evaporator air flow reduction	Condenser water flow reduction
Subcooling	Decrease	Not significant	Increase
T_{cond}	Decrease	Depends on T_{out}	Decrease, except for 10 °C
T_{evap}	Decrease	Decrease	Decrease
Freq	Increase	Increase	Small increase
EEV opening	Increase	Small increase	Not significant
$T_{air, out}$	-	Decrease	-

Table 3: Main effects of faults on the variables of the HP

Compared to fixed-speed HP, it is more difficult to characterize faults with variable speed because operating conditions affect a lot the evolution of the variables for a same fault. Also, the direct impact on the performances is reduced thanks to the compensation of the compressor. The effects in red are the ones that could allow to discriminate one fault from another. Subcooling is very interesting data to analyse as it reacts significantly and differently for condenser fouling and refrigerant charge reduction. This implies that a measurement of the condensing temperature should be made. Evaporating temperature and evaporator air outlet

temperature seem very relevant in order to detect evaporator fouling. Having access to the compressor rotating frequency is very interesting in order to see how the HP reacts to faults. This measurement can be made when measuring the compressor power input.

Thus, it could be possible to detect and identify a fault from the measurements of some variables, as long as the impact is significant enough to be measurable. To go further and in order to implement an in-situ fault detection and diagnostics method, first it would be needed to make these measurements possible on field, and then, the reference values in any operating condition should be known, from physical or statistical modelling for example.

6. CONCLUSION

The experiments presented in this paper show that different faults have different impacts on the functioning variables of the HP tested. Observing a single variable might not be enough to characterize a particular fault, but a combination of the impacts on different variables can be useful to differentiate one fault from another. Therefore, the knowledge of these impacts is necessary to be able to detect faults.

This experimental work is a step towards the development of a fault detection and diagnostics (FDD) tool for residential inverter-driven HP, but it will require some other studies to make the correlations between the faults and their impacts compatible from one HP to another, especially because there can be some differences of control from one manufacturer to another, and for other types of heat pumps. Also, the HP studied uses a small plate heat exchanger as a condenser, which makes it very sensitive to refrigerant charge variations. A bigger HP or an air-to-air HP might not be as sensitive.

Moreover, for the implementation of an FDD tool on field, it will be necessary to identify what measurements can be made easily outside a laboratory. For example, measuring the refrigerant mass flow rate is challenging, that is why the in-situ refrigerant method (Tran et al. 2012 and Niznik 2017) can be very useful, to avoid the need of a heavy instrumentation.

The measured values must be compared with reference values, or unfaulted values. Knowing them can be quite challenging as the functioning variables depend on the operating conditions. A further study of existing faults detection and diagnostics algorithms, and the development of a tool to learn these values should be made, for example based on physical modelling or machine-learning.

REFERENCES

Bory, D. (2008). *Analysis and simulation of defects of operation for air conditioning audit.* (Doctoral dissertation, Mines ParisTech, Paris, France). Retrieved from https://pastel.archives-ouvertes.fr/pastel-00004297

Goossens, M., Teuillières, C., Rivière, P., Cauret, O. & Marchio, D. (2017). An Instrumented Method for the Evaluation of Compressor Heat Losses in Heat Pumps On-Field, *Proceedings of the 12th IEA Heat Pump Conference, Rotterdam, Netherlands.*

Kim, W., & Braun, J. E. (2012a). Evaluation of Virtual Refrigerant Mass Flow Sensors. *International Refrigeration and Air Conditioning Conference*. Retrieved from http://docs.lib.purdue.edu/iracc/1245

Kim, W., & Braun, J. E., (2012b). Virtual Refrigerant Mass Flow and Power Sensors for Variable-Speed Compressors. *International Refrigeration and Air Conditioning Conference*, 1–8.

Kim, W., & Braun, J. E. (2015). Extension of a virtual refrigerant charge sensor. *International Journal of Refrigeration*, *55*, 224–235.

Li, H., & Braun, J. E. (2007). Decoupling features and virtual sensors for diagnosis of faults in vapor compression air conditioners. *Int. J. of Refrig., 30,* 546-564.

Madani, H. (2016). Smart Fault Detection and Diagnosis for Heat Pump Systems, *Refrigeration Science and Technology*, International Institute of Refrigeration, 2015, p. 3703-3710

Madani, H. (2014). The common and costly faults in heat pump systems, *Proceedings of the 6th International Conference on Applied Energy – ICAE 2014* (pp. 1803-1806). Taipei City: Energy Procedia.

Mehrabi, M., & Yuill, D. (2017a). Generalized effects of refrigerant charge on normalized performance variables of air conditioners and heat pumps. *International Journal of Refrigeration*, *76*, 367–384.

Mehrabi, M., & Yuill, D. (2017b). Generalized effects of faults on normalized performance variables of air conditioners and heat pumps. *International Journal of Refrigeration*, *85*, 409–430.

Niznik, M. (2017). *Improvement and integration of the in-situ heat pump performance assessment method* (Doctoral dissertation, PSL Mines ParisTech, Center for Energy efficiency of Systems, Paris, France). Retrieved from https://pastel.archives-ouvertes.fr/tel-01753394

Noël, D., Teuillières, C., Rivière, P., Cauret, O., & Marchio, D. (2018). Non-Intrusive Performance Assessment Method for Heat Pumps: Experimental Validation and Robustness Evaluation Facing Faults. *International Refrigeration and Air Conditioning Conference*

Tran, C.T. (2012) Méthodes de mesure in situ des performances annuelles des pompes à chaleur air/air résidentielles (Doctoral dissertation, Mines ParisTech, Paris, France). Retrieved from https://hal.archives-ouvertes.fr/pastel-00765206

Tran, C. T., Rivière, P., Marchio, D., & Arzano-Daurelle, C. (2013). In situ measurement methods of air to air heat pump performance. *International Journal of Refrigeration*, *36*(5), 1442–1455.

Wichman, A., & Braun, J. E. (2009). Fault detection and diagnostics for commercial coolers and freezers. *HVAC and R Research*, *15*(1), 77–99.

Yuill, D. P., Cheung, H., & Braun, J. E. (2014). Evaluating Fault Detection and Diagnostics Tools with Simulations of Multiple Vapor Compression Systems. *Proceedings of the International Refrigeration and Air Conditioning Conference*.

NOMENCLATURE

A	area	(m²)
C_{oil}	oil concentration	
$c_{p,oil}$	oil specific heat	(J/(kg.K))
D	compressor diameter	(m)
h	enthalpy	(J/kg)
k	fluid thermal conductivity	(W/(m.K))
L	lateral compressor length	(m)
$\dot{m}$	mass flow rate	(kg/s)
$\overline{Nu}$	Nusselt number	
$\dot{Q}$	thermal power	(W)
T	temperature	(K)
$\dot{W}$	electric power	(W)
σ	Stefan-Boltzmann constant	(W/(m².K⁴))

Subscript

Amb	ambient air
avg	average
cond	condenser
comp	compressor
D,1	top surface of the compressor
D,2	bottom surface of the compressor
in	inlet
L	lateral side of the compressor
out	outlet
r	refrigerant
surf	surface of the compressor
tot	total

Abbreviations

CA	condenser fouling
CFD	computational fluid dynamics
CH	refrigerant charge fault
COP	coefficient of performance
EA	evaporator fouling
EEV	electronic expansion valve
FI	fault intensity
FIR	fault impact ratio
Freq	compressor frequency
FXO	fixed-orifice expansion valve
HP	heat pump
SC	subcooling
TXV	thermostatic expansion valve